Improved parametrization of K^{+} production in p-Be collisions at low energy using Feynman scaling

C. Mariani, G. Cheng, J. M. Conrad, and M. H. Shaevitz

Phys. Rev. D **84**, 114021 — Published 20 December 2011

DOI: 10.1103/PhysRevD.84.114021

Improved Parameterization of K^+ Production in p-Be Collisions at Low Energy Using Feynman Scaling

C. Mariani,[1] G. Cheng,[1] J. M. Conrad,[2] and M. H. Shaevitz[1]

[1] *Columbia University, New York, NY 10027*

[2] *Department of Physics, Massachusetts Institute of Technology, Cambridge, Massachusetts 02139, USA*

This paper describes an improved parameterization for proton-beryllium production of secondary K^+ mesons for experiments with primary proton beams from 8.89 to 24 GeV/c. The parameterization is based on Feynman scaling in which the invariant cross section is described as a function of x_F and p_T. This method is theoretically motivated and provides a better description of the energy dependence of kaon production at low beam energies than other parameterizations such as the commonly used "Modified Sanford-Wang" model. This Feynman scaling parameterization has been used for the simulation of the neutrino flux from the Booster Neutrino Beam at Fermilab and has been shown to agree with the neutrino interaction data from the SciBooNE experiment. This parameterization will also be useful for future neutrino experiments with low primary beam energies, such as those planned for the Project X accelerator.

PACS numbers: 13.25.Es,13.87.Ce

I. INTRODUCTION

This paper describes a parameterization for inclusive production of secondary K^+ mesons in proton-beryllium collisions,

$$p + Be \rightarrow K^+ + X, \tag{1}$$

for experiments with low primary proton beam energies ranging in kinetic energy from below 9 to 24 GeV. The parameterization is based on Feynman scaling(F-S) [1], in which the invariant cross section is described as a function of transverse momentum, p_T, and a scaling variable, $x_F = p_{||}^{CM}/p_{||}^{CM\ max}$. Various scaling parameterizations are known to describe data well above ∼20 GeV [2, 3]. In this paper, we show that the F-S form describes data down to 8.89 GeV/c beam momentum. This result provides an alternative model to the traditional "Modified Sanford-Wang" [4, 5] parameterization used to describe secondary production at low primary proton beam momentum. The results from this F-S analysis have been used in the neutrino flux parameterization of the Booster Neutrino Beam (BNB) at Fermilab and has been checked against measurements by the SciBooNE experiment [6]. This parameterization will be useful for future neutrino experiments using low primary proton beam energies.

The primary motivation for this work was the simulation of neutrinos in the BNB line. This line provides neutrinos for the MiniBooNE [7] and SciBooNE [6] experiments, as well as possible future experiments, including the upcoming MicroBooNE [8] experiment. In this beam line, protons with 8 GeV kinetic energy are directed onto a 1.8 interaction length beryllium target. The charged pions and kaons which are produced are focused by a magnetic horn into a 50 m decay region, where they subsequently decay to produce neutrinos. The average energy of π^+ (K^+) that decay to neutrinos in the MiniBooNE detector acceptance is 1.89 (2.66) GeV. Therefore 37.6% (92.1%) of the particles decay before the end of the 50 m long decay region. The most relevant decay modes for MiniBooNE are $\pi^+ \rightarrow \mu^+\nu_\mu$, $K^+ \rightarrow \mu^+\nu_\mu$, which produce 99.4% of the neutrino beam, and $K^+ \rightarrow \pi^0 e^+\nu_e$, $\mu^+ \rightarrow e^+\bar{\nu}_\mu\nu_e$, $K_L^0 \rightarrow \pi^- e^+\nu_e$, and $K_L^0 \rightarrow \pi^+ e^-\bar{\nu}_e$, which produce the remaining 0.6%.

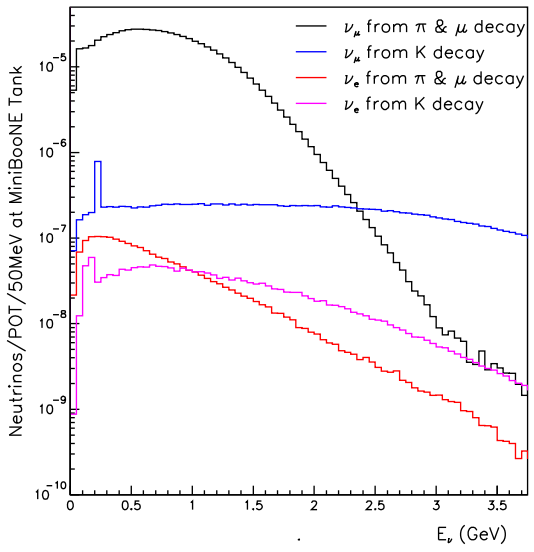

FIG. 1. Predicted ν_μ and ν_e flux spectrum from decaying pions, kaons, and muons for the BNB and SciBooNE and MiniBooNE experiments.

Figure 1 shows the predicted flux for the BNB line at the MiniBooNE detector. While the flux is predominately due to π^+ decay, the K^+ decay is the dominant source above 2 GeV. The ν_e flux from kaon decay contributes one of the important backgrounds for neutrino oscillation searches looking for ν_e appearance. In addition, the kaon neutrino flux provides an interesting source

of high energy events for experiments on the BNB line for studying neutrino cross sections. Therefore, it is important for the BNB line experiments to have a good first-principles prediction of K^+ production.

A first-principles prediction for K^+ production is obtained from fitting data from secondary production experiments with primary beam momentum ranging from 8.89 to 24 GeV/c. Nine data sets are considered, but only seven are used in the fit as it will be explained in Section III. Because these data are taken at a range of beam energies, the data must be fit to a parameterization including changes with beam momentum in order to scale the result to the 8.89 GeV/c of the BNB line momentum.

A. Feynman Scaling Formalism

Over the past several decades, many experiments have made measurements of particle production by protons of various energies on many different nuclear targets. These data have been used to study the phenomenology of particle production and have led to several scaling laws and quark counting rules. For inclusive particle production, Feynman put forward a theoretical model [1] where the invariant cross section is only a function of x_F and p_T. The invariant cross section is related to the commonly used differential cross section by:

$$\frac{d^2\sigma}{dpd\Omega} = \frac{p^2}{E}E\frac{d^3\sigma}{dp^3}. \quad (2)$$

Defining

$$E\frac{d^3\sigma}{dp^3} = AF(x_F, p_T), \quad (3)$$

this leads to:

$$\frac{d^2\sigma}{dpd\Omega} = \frac{p^2}{E}A\ F(x_F, p_T). \quad (4)$$

A is a factor and F is the F-S function that depends on x_F and p_T. The quantity $p_{||}^{CM\ \max}$, which appears in the denominator of the definition of x_F, depends upon the particle being produced and is derived from the exclusive channels given in Table I.

Feynman scaling has been demonstrated for secondary meson production at primary beam energies above ∼15 to 20 GeV [2, 3, 9]; this paper demonstrates the validity of F-S at lower primary beam energies for K^+ production. One might expect F-S to be a better parameterization of K^+ production than the "Modified Sanford-Wang" formalism for two reasons. First, the F-S parameterization properly accounts for the kinematic effects of the large kaon mass where even at $x_F = 0$, the outgoing kaon can have a significant laboratory momentum. Second, the functional form of the parameterization typically has peak production at $x_F = 0$. This is in contrast to the "Modified Sanford-Wang" formalism, where the production rate continues to grow as x_F becomes more negative.

Produced Hadron	Exclusive Reaction	M_X (GeV/c^2)	$\sqrt{s_{thresh}}$ (GeV)	E_{thresh}^{beam} GeV
π^+	pnπ^+	1.878	2.018	1.233
π^-	pp$\pi^+\pi^-$	2.016	2.156	1.54
π^0	ppπ^0	1.876	2.011	1.218
K^+	$\Lambda^0 pK^+$	2.053	2.547	2.52
K^-	ppK^+K^-	2.37	2.864	3.434
K^0	pΣ^+K^0	2.13	2.628	2.743

TABLE I. Threshold production channels for proton + proton production of various mesons. The exclusive reaction is the final state with the minimum mass, M_X. $\sqrt{s_{thresh}}$ and E_{thresh}^{BEAM} are the threshold center of mass (CM) and laboratory energy.

B. Feynman Scaling Parameterization for the Particle Production Cross Section

The Feynman model can be used to describe the expected x_F and p_T dependence using theoretically inspired functions for these dependences. For the x_F dependence, a parameterization proportional to $\exp(-a\,|x_F|^b)$ or $(1-|x_F|)^c$ has the properties consistent with a flat rapidity plateau around $x_F = 0$. The expectation of a limited p_T range is provided by including exponential moderating factors for powers of p_T.

Using this guidance, a F-S parameterization has been developed to describe kaon production. In order to allow some coupling between the x_F and p_T distribution an additional exponential factor has been added that uses the product, $|p_T \times x_F|$. The c_i's are the seven coefficients of the F-S function. The kinematic threshold constraint for K^+ production is imposed by setting $\frac{d^2\sigma}{dpd\Omega}$ equal to zero for $|x_F| > 1$.

Including these factors, the final parameterization has the form:

$$\frac{d^2\sigma}{dpd\Omega} = \frac{p_K^2}{E_K}\left(E_K\frac{d^3\sigma}{dp_K^3}\right) = \left(\frac{p_K^2}{E_K}\right)c_1 \times$$
$$\times \exp\left[c_3\,|x_F|^{c_4} - c_7\,|p_T \times x_F|^{c_6} - c_2 p_T - c_5 p_T^2\right]. \quad (5)$$

C. The "Modified Sanford-Wang" Parameterization

Many neutrino experiments have used the "Modified Sanford-Wang" parameterization[4, 5] (S-W):

$$\frac{d^2\sigma}{dpd\Omega} = c_1 {p_K}^{c_2}(1 - \frac{p_K}{P_{BEAM} - c_9}) \times$$
$$\times \exp\left[\frac{-c_3 {p_K}^{c_4}}{{P_{BEAM}}^{c_5}} - c_6\theta_K(p_K - c_7 P_{BEAM} cos^{c_8}\theta_K)\right] \quad (6)$$

This functional form allows for some phenomenological parameterization of the variations associated with beam energy and process thresholds. As noted in one of the initial Sanford-Wang papers [4, 5], the coefficients for π^+ production are approximately given by: $c_2 = 0.5, c_4 = c_5 = 1.67$, and the $\cos\theta$ term is negligible. With these substitutions, the formula shows a close although not perfect relationship with F-S (see Eq. 5)

$$E\frac{d^3\sigma}{dp^3}^{Sanford-Wang} = A'\ F'(X)\ e^{-Cp_T}, \quad (7)$$

where

$$F'(X) = X^{1/2}(1 - X)e^{-BX^{5/3}} \quad (8)$$

and

$$X = \frac{p}{P_{BEAM}}. \quad (9)$$

Therefore, the S-W fits to the K^+ data will show only approximate consistency with F-S. At low beam energy, produced particle mass effects can become important. Table I gives the minimum mass channels, their invariant mass, and the beam energy threshold for different particle production processes. In the S-W formula, the parameter c_9 is included to approximately provide the kinematic limit for produced particle momentum. Investigations of the exact kinematic threshold for K^+ production show that the maximum p_K is approximately equal to $P_{BEAM} - P_{Diff}$ where P_{Diff} varies from 1.7 to 2.2 GeV as θ_K goes from 0 to 0.3 rad. One would therefore expect that c_9 would take on values similar to P_{Diff}. On the other hand, the factor $(1 - \frac{p_K}{P_{BEAM}-c_9})$ introduces violations of the scaling behavior away from this limiting region.

An additional problem with the S-W parameterization is that most of the function parameters (c_i) will be effectively fixed by the scaling constraints, and this will be limiting the flexibility of the function to match the x_F and p_T behavior. The parameter c_2, for example, should be close to unity to provide the conversion from invariant to differential cross section. The parameter c_9 needs to be approximately equal to 2.0 GeV to provide the maximum p_K dependence, and the parameters c_4 and c_5 should be equal in order to preserve a basic x_F dependence. Thus, the S-W parameterization has very little flexibility to fit the data distributions over the full kinematic range and therefore a formalism like Feynman scaling is required. In many of the following plots, we will compare prediction results coming from S-W and F-S parameterizations.

II. EXTERNAL DATA SETS AND KINEMATIC COVERAGE

Several K^+ production measurements have been made for beam momentum less than 25 GeV/c and are reported in Table II. Those experiments, except for Piroue, have beam momenta higher than the BNB value of 8.89 GeV/c although some of them such as Aleshin and Vorontsov are fairly close to the BNB beam momentum. The kaons that produce neutrinos in MiniBooNE span the kinematic region with -0.1< x_F <0.5 and 0.05< $p_T(GeV/c)$ <0.5 as shown in Figure 2, which is nicely covered by the experimental data sets listed in Table II. Of course, we are using the assumption that one can extrapolate these higher beam momentum data to the BNB energy value using a parameterization such as F-S. Thus, the first question to be answered is whether the data appears to follow these scaling parameterizations.

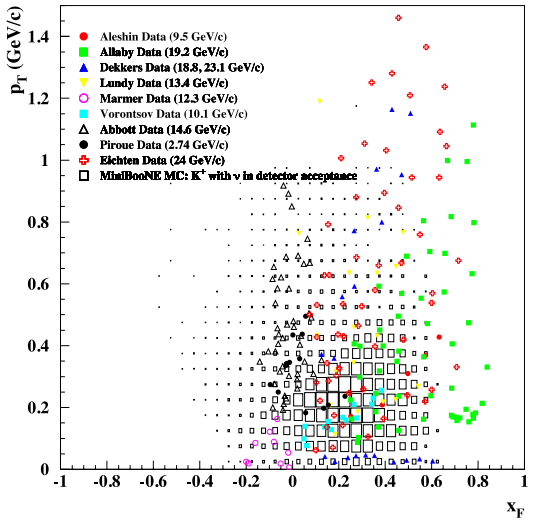

FIG. 2. Values of x_F and p_T for the data points of the various data sets in Table II. The distribution for kaons that produce ν_e events in the MiniBooNE detector is shown as open boxes.

The F-S hypothesis says that the invariant cross section $E\frac{d^3\sigma}{dp^3}$ should only depend on x_F and p_T. This hypothesis can further be tested by scaling all the data to a common beam momentum and checked by the behavior of the invariant cross section against the scaled value of p_K and θ_K. Figure 3 shows the invariant cross section for scaled kaon momentum and angle bins using the F-S assumption. For this plot, the data from each data set is converted first to x_F and p_T and then scaled to $p_K^{8.89}$ and $\theta_K^{8.89}$ for a 8.89 GeV/c beam momentum. For example, given a cross section point at P_{BEAM}=20 GeV/c with a given P_K and θ_K, one can calculate the x_F and p_T for this point. One can then find the equivalent p'_K and θ'_K that would have the same x_f and p_T at P_{BEAM}=8.89 GeV/c. As seen from the plots, the data appears to obey the scaling hypothesis reasonably well except for the Lundy, Piroue, and Vorontsov data sets. Due to the disagree-

K^+Data	Ref.	P_B(GeV/c)	P_K(GeV/c)	θ_K (rad)	x_F	p_T(GeV/c)	σ_{Norm}
Abbott	[10]	14.6	$2-8$	0.35−0.52	$-0.12-0.07$	$0.2-0.7$	10%
Aleshin	[11]	9.5	$3-6.5$	0.06	$0.3-0.8$	$0.2-0.4$	10%
Allaby	[12]	19.2	$3-16$	0−0.12	$0.3-0.9$	$0.1-1.0$	15%
Dekkers	[13]	18.8 , 23.1	$4-12$	0, 0.09	$0.1-0.5$	$0.0-1.2$	20%
Eichten	[14]	24.0	$4-18$	0−0.10	$0.1-0.8$	$0.1-1.2$	20%
Lundy	[15]	13.4	$3-6$	0.03, 0.07, 0.14	$0.1-0.6$	$0.1-1.2$	20%
Marmer	[16]	12.3	$0.5-1$	0, 0.09, 0.17	$-0.2--0.05$	$0.0-0.15$	20%
Piroue	[17]	2.74	$0.5-1$	0.23, 0.52	$-0.3-1.0$	$0.15-0.5$	20%
Vorontsov	[18]	10.1	$1-4.5$	0.06	$0.03-0.5$	$0.1-0.25$	25%

TABLE II. Data sets for K^+ production with proton momentum lower than 24 GeV/c. P_B indicates the beam momentum and σ_{Norm} gives the normalization error for the experimental data.

ments of the Lundy and Piroue data, these data sets are not included in the fits described below. The Vorontsov data appears to agree in shape with the other data sets but has an anomalous normalization. Data sets not included in the fits are not discarded. They are compared separately to the fit results, as explained below.

III. FEYNMAN SCALING AND SANFORD-WANG MODEL FITS TO THE K^+ EXTERNAL DATA SETS

Under the assumption that the experimental data follow the Feynman or S-W scaling models, we can determine a parameterization that best fits these data sets. The various production data sets are used as input to a fit for the scaling function parameters that best describe the data. The fit uses a χ^2 minimization technique using Minuit [19] to perform the numerical minimization. Each experiment is allowed to have an independent normalization parameter that is constrained by the published normalization uncertainty. The fit minimizes the following function for an experiment j:

$$\chi_j^2 \;=\; \left[\sum_i \frac{(N_j \times SF_i - Data_i)^2}{(f\times\sigma_i)^2}\right] + \frac{(1-N_j)^2}{\sigma_{N_j}^2}, \quad (10)$$

where i is the (P_K,θ_K) bin index, SF is the scaling function prediction evaluated at the given $(P_{BEAM}, \theta_K, p_K)$, $Data_i$ is the measurement at a given $(P_{BEAM}, \theta_K, p_K)$, σ_i is the data error for measurement i, f is the scaling factor to bring the $\chi^2/d.o.f. = 1$, N_j is the normalization factor for experiment j, σ_{N_j} is the normalization uncertainty for experiment j, and d.o.f. indicates degree of freedom. The total χ^2 for external data sets is then the sum over the experiments of the individual χ_j^2 values,

$$\chi^2 = \sum_j \chi_j^2. \quad (11)$$

The χ^2 is minimized in order to obtain the best values and uncertainties for the parameterization coefficients c_j, given in Eq. 5 (or 6, and for the normalization factors N_j). The uncertainties on the fit values at 1σ are determined from a $\Delta\chi^2 = 1$ change with respect to χ^2_{min} and the fit also yields a covariance matrix that can be used to propagate correlated errors associated with the parameterization of the cross section.

A F-S fit to all the experimental data sets with 0.0< $P_K^{8.89}(GeV/c)$ <6.0 gives a χ^2/d.o.f. equal to 4.03 with large χ^2 contributions from data with $P_K^{8.89}$ <1.2 GeV/c and $P_K^{8.89}$ >5.5 GeV/c. Therefore for the final scaling fits, the points with the larger pull terms, defined as $((N_j \times SF_i - Data_i)/\sigma_i)$, have been eliminated by only using data with 1.2< $P_K^{8.89}(GeV/c)$ <5.5.

The 1.2 GeV/c cut effectively removes data at negative x_F where the nuclear environment starts to play an important role. This cut also eliminates all the Marmer data points.

With all of these requirements, the χ^2/d.o.f. for the F-S fit is reduced to 2.28. The uncertainties for the fitted cross section need to be corrected for this χ^2/d.o.f., which is larger than 1.0. This is accomplished by scaling up the errors of each of the data points by $\sqrt{\chi^2/d.o.f.}$ before doing the fit. Figure 4 shows the pull terms for the seven parameter F-S fit where the errors have been scaled up by this $\sqrt{\chi^2/d.o.f.} = \sqrt{2.28}$ =1.51.

A S-W fit to all the experimental data has been performed as well. To be able to directly compare the S-W with the F-S fit we have included in the S-W fit only data with 1.2< $P_K^{8.89}(GeV/c)$ <5.5. The χ^2/d.o.f. for the S-W fit is equal to 6.05.

IV. COMPARISON OF FEYNMAN SCALING TO SANFORD WANG RESULTS AND NEUTRINO PREDICTIONS

Tables III and IV report the final fit values for the coefficients and the normalization factors for the F-S and S-W parameterizations respectively. Figures 5 and 6 show the fit function curves for the F-S and S-W parameterizations as compared to the data. The fits are stable with respect to parameter starting values and yield positive definite covariance matrices. The error bands in

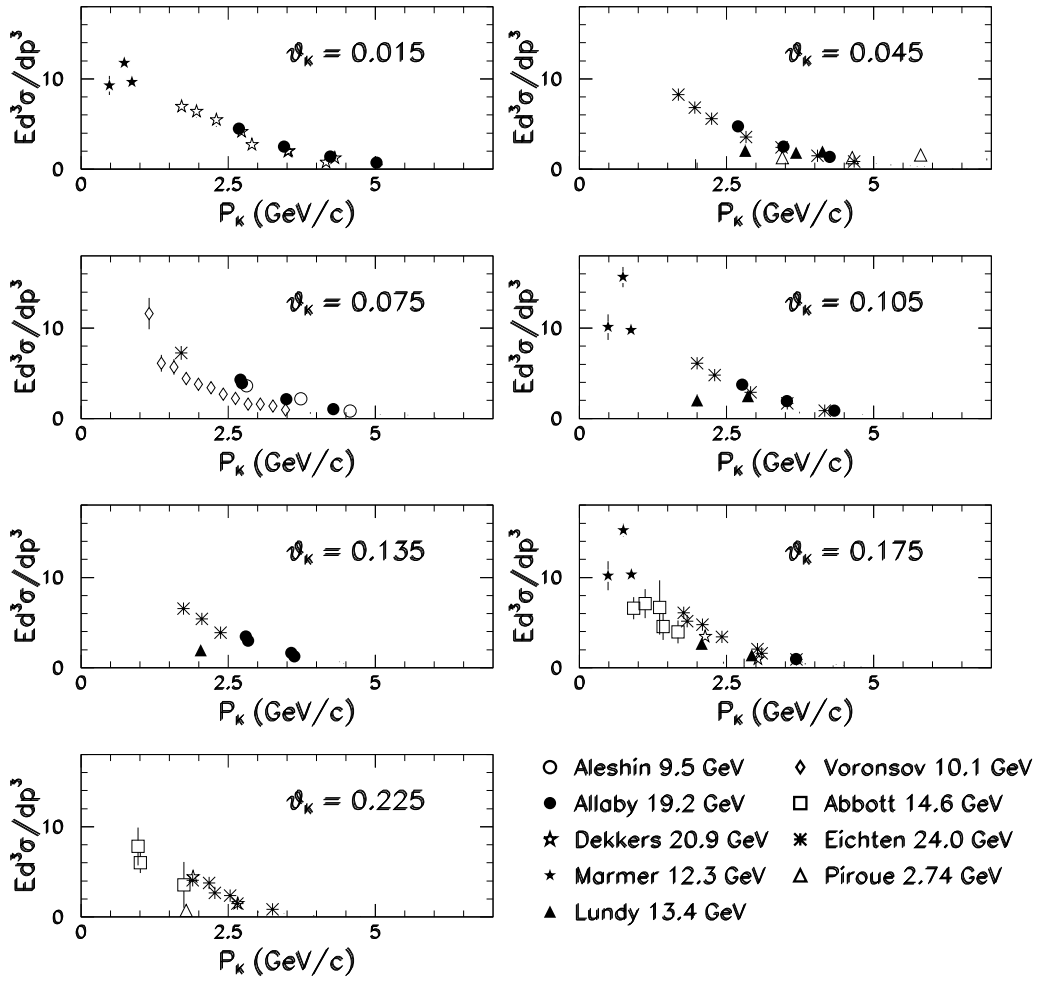

FIG. 3. K^+ production data sets scaled to the MiniBooNE beam momentum of 8.89 GeV/c using F-S. The Y-axis units are $(mb \times c^3/GeV^2)$. The production angle varies from 0 to 0.225 *rad*.

Figures 5 and 6 are determined by propagating the covariance matrix for the c_j parameters to the invariant cross section errors.

As seen from the plots, the F-S function gives a very good description of the data over the full kaon momentum range used in the fit and has a reasonable χ^2/d.o.f. = 2.3. Below 1.2 GeV/c, the F-S prediction has some disagreement with a few the of the Marmer (not included in the fit) and Abbott data points but in general is also fitting that well in that region. The normalization factors for the F-S fits are within 1σ of the quoted experimental error except for the Vorontsov data (see Table III). As mentioned above, the Vorontsov data shows a systematically low normalization with respect the other sets of scaled data. Therefore, for all the scaling fits, the Vorontsov data has only been used for shape information by giving the normalization a large uncertainty (500%).

In contrast, the S-W final fit parameterization has rather large discrepancies with the data in almost all regions and has a much larger χ^2/d.o.f. = 6.05. Additionally, the normalization factors given in Table IV are very much outside of the quoted experimental errors and, for example, the factors for Eichten and Allaby differ from 1.0 by 2 to 3σ.

Tables V and VI list the differential cross sections for several different kinematic points for kaon production. The uncertainties are obtained by propagating the covariance matrix for the c_j coefficients into the scaling function. The first three points in Table V and VI correspond to the mean kaon production points that produce electron neutrino of 0.35, 0.65, and 0.95 GeV in MiniBooNE. The fourth point corresponds to the kaon kinematics that produce average energy neutrinos from all kaon decays (called the "kaon sweet spot"), and the fifth point is associated with the mean kaon kinematics for the highest energy kaon-decay muon neutrinos ob-

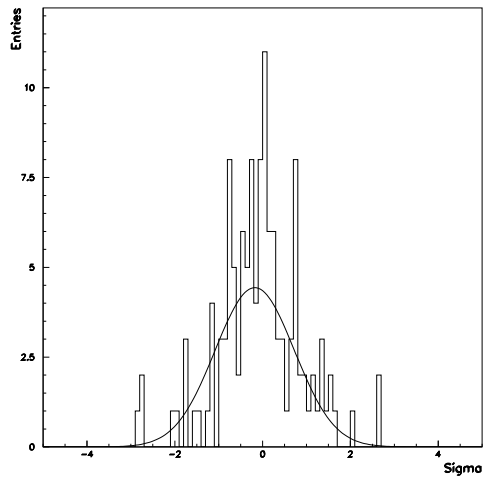

FIG. 4. Values of the pull terms, $(N_j \times SF_i - Data_i)/\sigma_i$, for each data point for the F-S fit for 1.2< $P_K^{8.89}(GeV/c)$ <5.5. The data errors, σ_i, have been scaled up by $\sqrt{\chi^2/d.o.f.} = \sqrt{2.28} = 1.51$. The Gaussian fit gives a $\chi^2/number\ of\ degree\ of\ freedom = 35.51/35$, with a mean value = (-0.18 ± 0.11) and sigma = (0.90 ± 0.17).

Feynman Scaling	1.2< $P_K^{8.89}(GeV/c)$ <5.5		
Fit	Value	Error	
c1	11.70	1.05	
c2	0.88	0.13	
c3	4.77	0.09	
c4	1.51	0.06	
c5	2.21	0.12	
c6	2.17	0.43	
c7	1.51	0.40	Input Error
Aleshin	1.09	0.07	0.10
Allaby	1.04	0.07	0.15
Dekkers	0.84	0.06	0.20
Vorontsov	0.53	0.04	5.00
Abbott	0.76	0.07	0.15
Eichten	1.00	0.07	0.15
χ^2/d.o.f. (no f)	2.28	$(d.o.f. = 119)$	

TABLE III. Results for the F-S fits to the K^+ data including a single normalization factor for each experiment. The data errors have been scaled up by a factor of $\sqrt{\chi^2/d.o.f.}$ =f= 1.51 when included in the fit but the χ^2/d.o.f. value listed is for the data without this scaling. d.o.f. indicates here degree of freedom and "no f" means no correction factor applied.

served in MiniBooNE. As seen from Table V and VI , the two parameterizations give much different results for the cross section values and uncertainties with the F-S fit giving a larger value by a factor 2 for the lowest energy neutrino bin at 0.35 GeV. The source of the this discrepancy is a large drop in the invariant cross section of the S-W parameterization at large angles.

Modified S-W	1.2< $P_K^{8.89}(GeV/c)$ <5.5		
Fit	Value	Error	
c1	14.89	1.89	
c2	0.91	0.13	
c3	12.80	7.46	
c4	2.08	0.35	
c5	2.65	0.50	
c6	4.61	0.10	
c7	0.26	0.01	
c8	10.63	7.06	
c9	2.04	0.01	Input Error
Aleshin	1.02	0.09	0.10
Allaby	0.74	0.09	0.15
Dekkers	0.57	0.08	0.20
Vorontsov	0.42	0.04	5.00
Abbott	1.38	0.11	0.15
Eichten	0.59	0.08	0.15
χ^2/df (no f)	6.05	$(d.o.f. = 117)$	

TABLE IV. Results for the S-W scaling fits to the K^+ data including a single normalization factor for each experiment. The data errors have been scaled up by a factor of $\sqrt{\chi^2/d.o.f.}$ =f= 2.46 when included in the fit but the χ^2/d.o.f. value listed is for the data without this scaling. d.o.f. indicates here degree of freedom and "no f" means no correction factor applied.

	$P_K^{8.89}$ (GeV/c)	θ_K (rad)	$\sigma_{K\ prod}$ (mb)
$E_\nu = 0.35$ GeV	1.52	0.213	9.37 ± 0.73 (7.8%)
$E_\nu = 0.65$ GeV	2.07	0.127	10.69 ± 0.75 (7.0%)
$E_\nu = 0.90$ GeV	2.45	0.103	10.22 ± 0.71 (6.9%)
Kaon Sweet Spot	2.80	0.106	8.67 ± 0.60 (6.9%)
HE ν_μ Events	4.30	0.055	4.73 ± 0.33 (7.0%)

TABLE V. Differential cross section values for various kinematic points for the 1.2< P_K <5.5 GeV/c F-S fit. The first three results are for the average kaon kinematics that give electron neutrinos with the given energy. The fourth result is the previous point used for a kaon sweet spot. The last result is for the average kaon kinematics associated with highest energy ν_μ events in MiniBooNE.

	$P_K^{8.89}$ (GeV/c)	θ_K (rad)	$\sigma_{K\ prod}$ (mb)
$E_\nu = 0.35$ GeV	1.52	0.213	4.25 ± 0.77 (18%)
$E_\nu = 0.65$ GeV	2.07	0.127	8.99 ± 1.34 (15%)
$E_\nu = 0.90$ GeV	2.45	0.103	9.91 ± 1.43 (14%)
Kaon Sweet Spot	2.80	0.106	7.73 ± 1.13 (15%)
HE ν_μ Events	4.30	0.055	5.24 ± 0.84 (16%)

TABLE VI. Differential cross section values for various kinematic points for the 1.2< P_K <5.5 GeV/c S-W scaling fit. The first three results are for the average kaon kinematics that give electron neutrinos with the given energy. The fourth result is the previous point used for a kaon sweet spot. The last result is for the average kaon kinematics associated with highest energy ν_μ events in MiniBooNE.

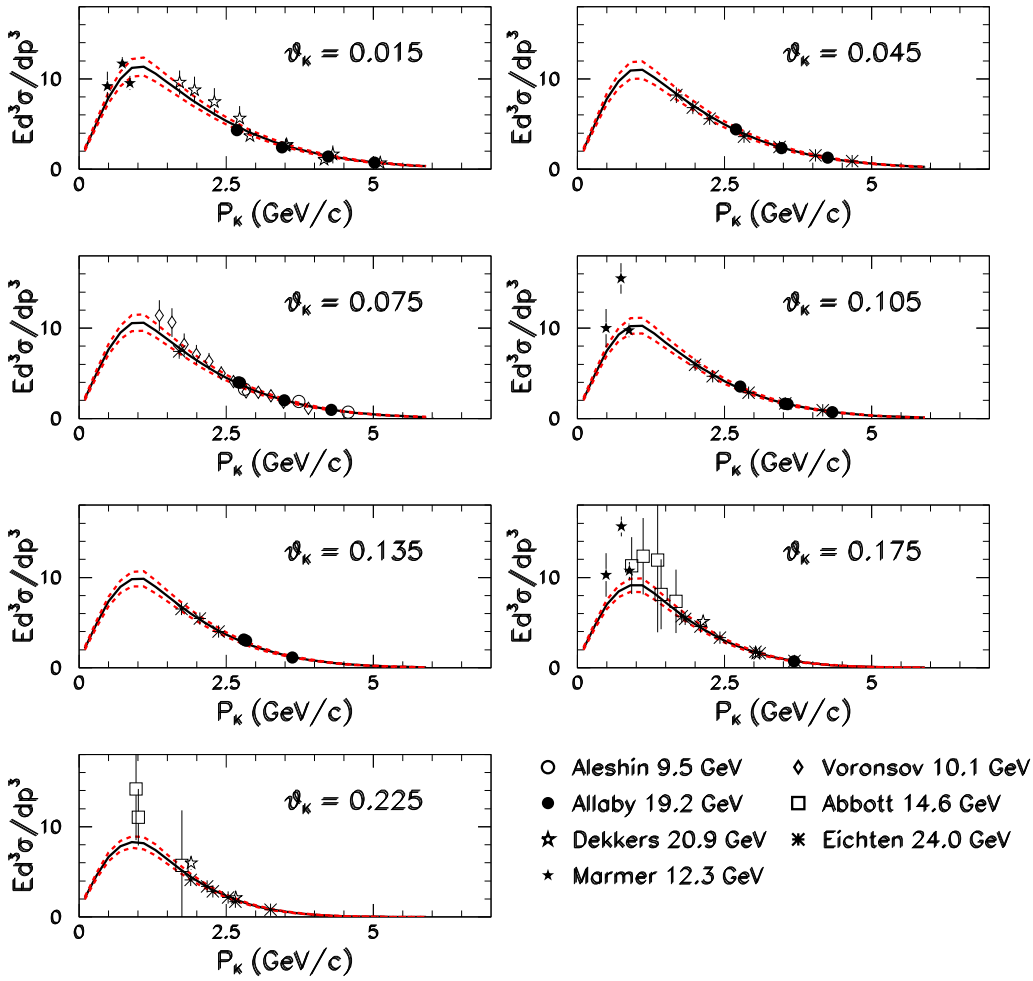

FIG. 5. Invariant kaon production cross section in $mb \times c^3/GeV^2$ versus kaon momentum for all data along with the results of the F-S fit to data with 1.2< $P_K^{8.89}(GeV/c)$ <5.5. The P_K, θ_K, and invariant cross section fits and the data points have been scaled to a beam momentum of 8.89 GeV/c assuming F-S and normalized according to the fit results. This plot shows data and fit results for various value of θ in bins from 0 to 0.225 rad. The three solid curves show the central value and 1σ uncertainty for the F-S fit.

The predictions for the size and kinematic dependence of the invariant differential cross section as function of K^+ momentum are quite different for the F-S and S-W parameterizations as shown in Figure 7, especially for low value of the K^+ momentum.

To illustrate the difference between the F-S and the S-W predictions, we have used an analytic simulation of the BNB neutrino beam line designed for the MiniBooNE experiment (described in Reference [20]). Table VII gives the comparison of the predicted ν_e event rate from $K^+ \to \pi e^+ \nu_e$ using the above F-S and S-W production parameterizations as calculated using this BNB simulation.

V. HIGH ENERGY PARAMETERIZATION

The hypothesis of F-S has also been verified to hold with different parameterizations over a wide range of primary proton beam energies (from 24 GeV to 450 GeV). In Bonesini *et al.* [2] data at higher proton energies has been empirically parameterized as a function of the transverse momentum (p_T) and the scaling variable $x_R = E^*/E^*_{max}$ where E^* is the energy of the particle in center-of-mass frame. The choice of these variables for the description of the invariant cross section (radial scaling) is motivated again by an assumed scaling behavior of the invariant cross section. The radial scaling variable is approximately equal to the F-S variable at high energy and has the property of never taking on a negative value. (A de-

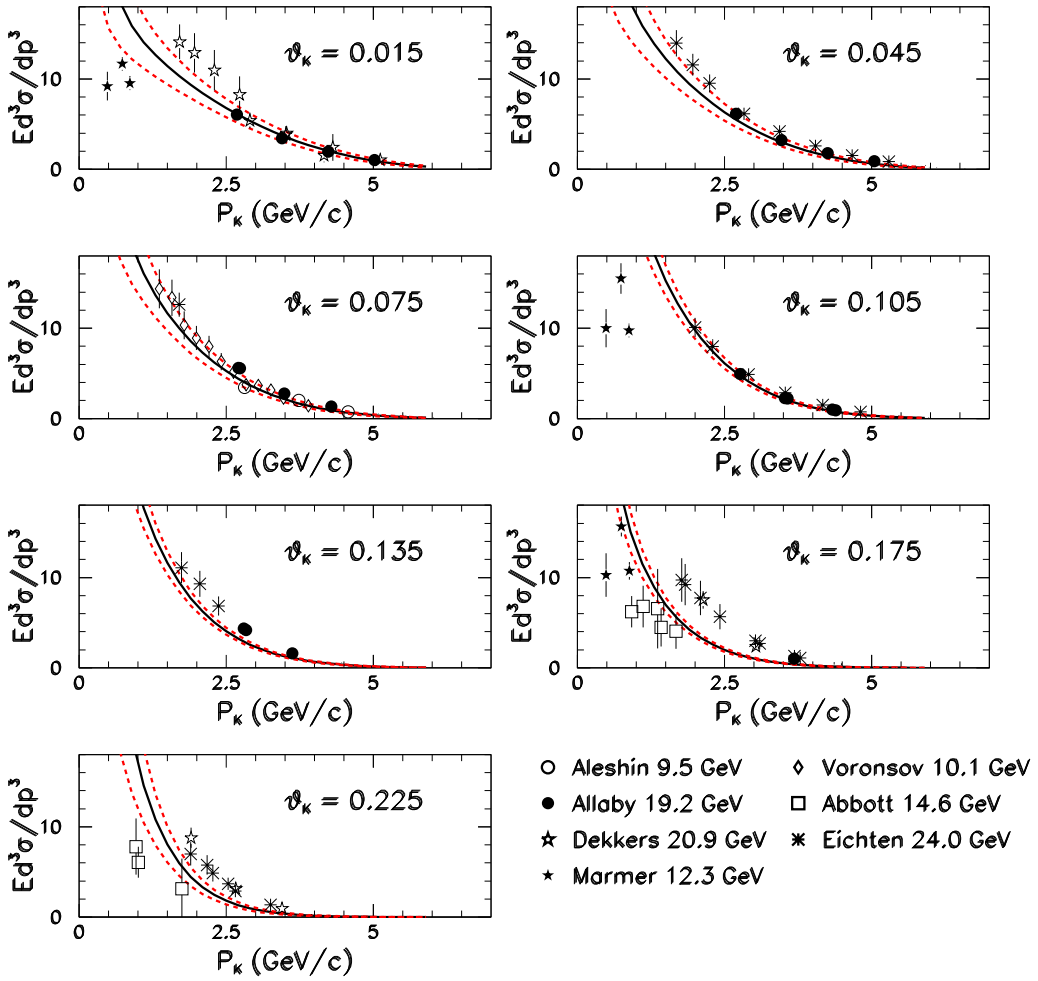

FIG. 6. Invariant kaon production cross section in $mb \times c^3/GeV^2$ versus kaon momentum for all data along with the results of the S-W scaling fit to data with 1.2< $P_K^{8.89}(GeV/c)$ <5.5. The P_K, θ_K, and invariant cross section fits and the data points have been scaled to a beam momentum of 8.89 GeV/c assuming S-W and normalized according to the fit results. This plot shows data and fit results for various value of θ in bins from 0 to 0.225 rad. The three solid curves show the central value and 1σ uncertainty for the S-W scaling fits.

θ_K	K^+_{e3} Feynman Scaling Fit			K^+_{e3} Sanford-Wang Fit		
Angular Bins(rad)	All E_ν(GeV)	<1 GeV	>2 GeV	All E_ν(GeV)	<1 GeV	>2 GeV
0.015	36.7	2.6	18.0	43.4	3.3	19.3
0.045	92.5	8.4	35.9	111.0	12.0	35.9
0.075	110.5	13.7	27.0	141.3	22.6	26.5
0.105	96.8	17.2	4.4	138.3	32.6	4.1
0.135	59.1	21.8	0.0	100.5	45.8	0.0
0.175	39.4	32.4	0.0	83.7	73.9	0.0
0.225	21.9	21.9	0.0	56.8	56.8	0.0
Total	476.6	137.9	85.3	731.2	303.4	85.9

TABLE VII. Electron neutrino event rate in MiniBooNE for 5.0×10^{20} proton on target for K^+_{e3} decays with F-S and S-W parameterizations. The events were calculated using MiniBooNE simulation and are for a beam radius less than 6.0 m. The different columns list the selected electron neutrino events for all E_ν, E_ν < 1 GeV, and E_ν > 2 GeV. Uncertainty in the neutrino event rate due to the F-S or S-W parametrization is 7% and 15% respectively as described in Table V and VI.

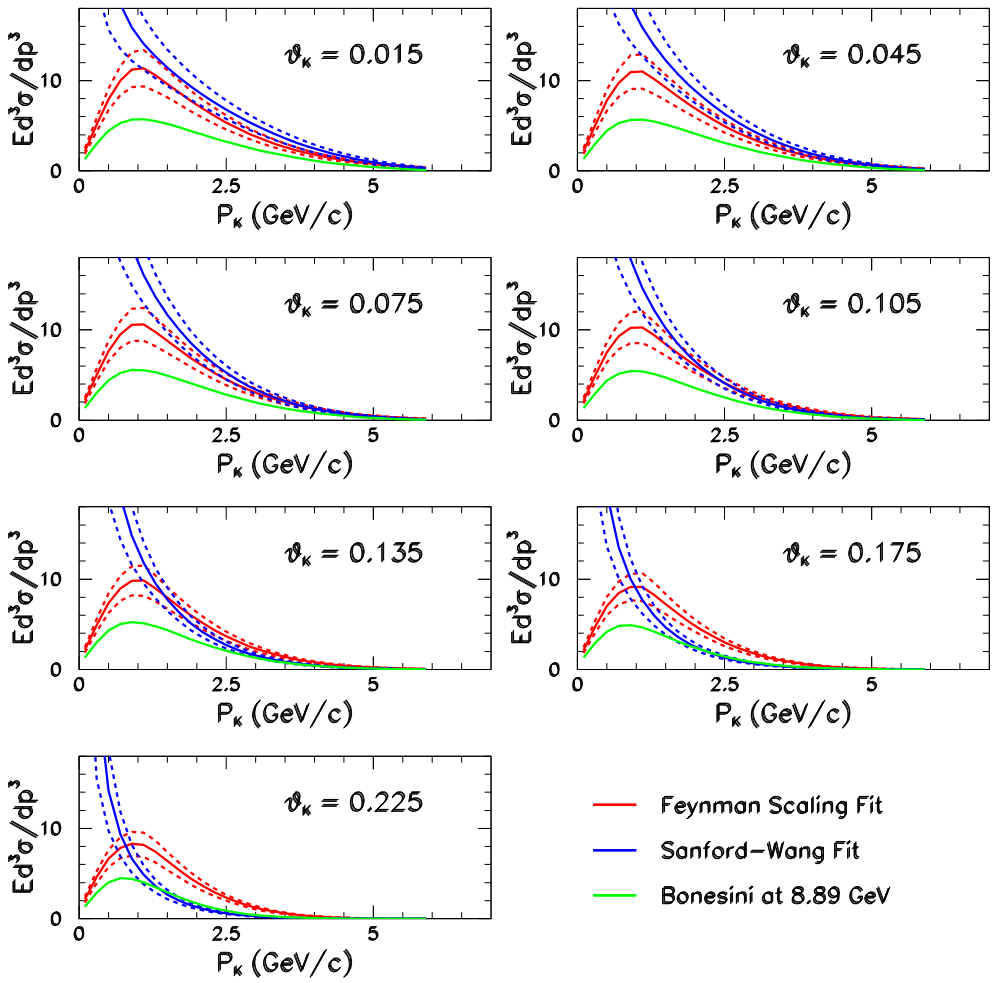

FIG. 7. Invariant kaon production cross section in units of $mb \times c^3/GeV^2$ versus kaon momentum in GeV/c for the S-W, F-S and radial scaling (Bonesini)[2] parameterizations for a beam momentum of 8.89 GeV/c. The results are shown for various θ bins from 0 to 0.225 rad. The three solid curves, respectively for the F-S and S-W fits, show the central value and 1σ uncertainty for each of the fits.

tailed comparison of radial scaling and F-S can be found in [3, 21], where the authors compare different models with the production data at different energies down to about 24 GeV.)

Bonesini *et al.*[2] has obtained an empirical parameterization based on radial scaling fits to data collected with 400 GeV/c and 450 GeV/c protons incident on a Be target. The results from this parameterization are compared in Figure 7 to the predictions of F-S and S-W models at a proton momentum of 8.89 GeV/c. As seen from Figure 7, this radial scaling model underestimates K^+ production at a beam momentum of 8.89 GeV/c by more than a factor of two even though the parameterization describes well the high proton momentum data (>24 GeV/c) [2].

VI. THE SCIBOONE K^+ MEASUREMENTS

The SciBooNE collaboration has reported a measurement [22] for K^+ production in the BNB with respect to the Monte Carlo (MC) beam simulation. The SciBooNE experiment collected data in 2007 and 2008 with neutrino (0.99×10^{20} protons on target (POT)) and antineutrino (1.53×10^{20} POT) beams in the Fermilab BNB line. The SciBooNE detector is located 100 m downstream from the neutrino production target. The flux-averaged mean neutrino energy is 0.7 GeV in neutrino running mode and 0.6 GeV in antineutrino running mode

The SciBooNE detector consists of three detector components; SciBar, Electromagnetic Calorimeter (EC) and Muon Range Detector (MRD). SciBar is a fully active and fine grained scintillator detector that consists of 14,336 bars arranged in vertical and horizontal planes. SciBar is capable of detecting all charged particles and performing dE/dx-based particle identification. The EC is located downstream of SciBar. The detector is a spaghetti calorimeter with thickness of 11 radiation lengths and is used to measure π^0 and the intrinsic ν_e component of the neutrino beam. The MRD is located downstream of the EC in order to measure the momentum of muons up to 1.2 GeV/c with range. It consists of 2-inch thick iron plates sandwiched between layers of plastic scintillator planes.

In the SciBooNE experiment, particle production is simulated using the methods described in Ref. [20]. The production of K^+ is simulated using the F-S formalism as described in Section I A with the coefficients reported in Table III. The predicted double differential cross section at the mean momentum and angle for kaons which produce neutrinos in SciBooNE ($P_K = 3.87$ GeV/c and $\theta_K = 0.06$ rad) is

$$\frac{d^2\sigma}{dpd\Omega} = (6.3 \pm 0.44)\ mb/(GeV/c \times sr). \quad (12)$$

The error on the double differential cross section prediction using the F-S parametrization at the SciBooNE p_K and θ_K is 7%. The SciBooNE and MiniBooNE collaboration have adopted a conservative error of 40%. This larger error was chosen because of the uncertainties in extrapolating the K^+ prediction data from high to low proton beam energy using the F-S and S-W models as explained in References [20, 22].

A. SciBooNE K^+ Production Measurement

The SciBooNE data can be used as an additional constraint in fits to K^+ production cross sections. In SciBooNE, neutrinos from K^+ decay are selected using high energy ν_μ interactions within the volume of the SciBar detector. The high-energy selection is accomplished by isolating charged current interactions that produce a muon that crosses the entire MRD. This sample is further divided into three sub-samples based on whether 1, 2, or 3 reconstructed SciBar tracks are identified at the neutrino interaction vertex in the SciBar detector. Since the reconstruction of the energy of the muon is not possible because the muon exits the MRD detector, the reconstructed muon angle relative to beam axis is used as the primary kinematic variable to separate neutrinos from pion and kaon decay. The values for $\frac{d^2\sigma}{dpd\Omega}$ for neutrino, antineutrino, and combined data mode running are given in Table VIII along with the mean energy and angles for the corresponding K^+ samples. The F-S and S-W prediction values are obtained using the parametrizations described in Section I A and I C along with the parameters listed in Table III and IV.

	E_{K^+} (GeV)	θ_{K^+}(rad)	$\frac{d^2\sigma}{dpd\Omega}$ (mb/(GeV/c × sr)
ν-mode	3.81±0.03	0.07±0.01	5.77±0.83
$\bar{\nu}$-mode	4.29±0.06	0.03±0.01	3.18±1.94
$\nu + \bar{\nu}$-mode	3.90±0.03	0.06±0.01	5.34±0.76
F-S prediction	3.90	0.06	6.30±0.44(7%)
S-W prediction	3.90	0.06	6.84±1.09(16%)

TABLE VIII. Measured $\frac{d^2\sigma}{dpd\Omega}$, mean energy, and mean angle (with respect to proton beam direction) for the selected K^+ in neutrino, antineutrino, and the combined neutrino and antineutrino samples using MiniBooNE MC. Errors on the mean energy and mean angle values correspond to the error on the mean for the relative distributions. F-S and S-W predictions are also reported at the mean SciBooNE K^+ energy and angle.

The K^+ momentum versus angle distribution for the 2-track SciBar sample in the simulation is shown in Figure 8.

Figure 8 shows the kinematics of the selected K^+

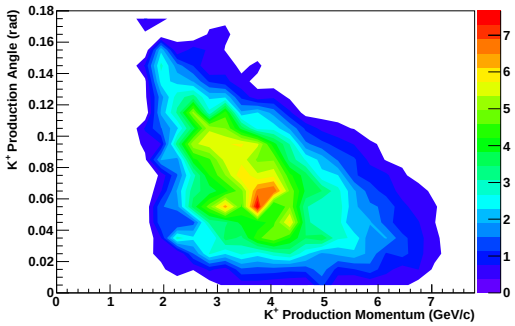

(a)Neutrino Sample

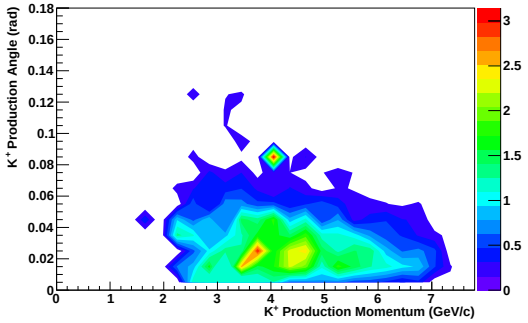

(b)Antineutrino Sample

FIG. 8. The true K^+ momentum versus angle distribution in the SciBooNE MC for neutrino-mode (on top) and antineutrino mode (on bottom) running. The unit for the color scale is number of events POT normalized.

events in SciBooNE, while Figure 9 shows the kinematical region as function of angle and momentum for K^+ mesons that produce ν_e events in MiniBooNE.

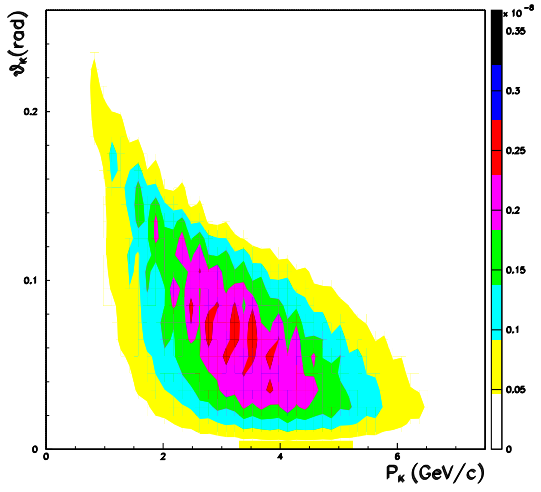

FIG. 9. Kinematical region as function of angle and momentum for the K^+ mesons that produce ν_e events in MiniBooNE. The unit for the color scale is number of events.

The SciBooNE measurement is a direct test of the extrapolation of parameterizations found from higher beam energies to the MiniBooNE beam energy. The predictions for the double differential cross section for the F-S and S-W models are reported in Table VIII and shows a good agreement with the SciBooNE measurement, a better agreement is found in the case of the F-S parametrization.

The SciBooNE K^+ production measurements can also be added to the F-S fit as additional external data using the following procedure. First we retrieve all the SciBooNE MC K^+ events with their θ_i and p_i for the neutrino and antineutrino sample. Then we calculate the following quantities:

$$N_i = \sum_i \frac{\frac{d^2\sigma}{dpd\Omega}(c_{fit}, \theta_i, p_i)}{\frac{d^2\sigma}{dpd\Omega}(c_{MC}, \theta_i, p_i)} \tag{13}$$

$$N_0 = \sum_i 1 \tag{14}$$

These quantities are then used at each fit step to build a pull term, defined in Eq. 15, to be added to the χ^2 of the fit.

$$pull - term_{\nu,\bar{\nu}} = \frac{\left(\frac{N_i}{N_0} - K^+_{prod,SB}\right)}{\left(error\ K^+_{prod,SB}\right)^2} \tag{15}$$

Each data point in θ_i and p_i is reweighted using the double differential cross section value for the current set of c_i coefficient of Eq. 5 computed at each step of the Minuit fit. The set of coefficient used in the MC is labeled as c_{MC}, the values of these coefficients is listed in Table III. The $K^+_{prod,SB}$ and $error\ K^+_{prod,SB}$ in the Eq. 15 are the values of the SciBooNE production measurement and error (see Table VIII), respectively.

Two separate pull terms are added to the fit χ^2 corresponding to the SciBooNE neutrino and antineutrino K^+ production measurements.

The results of scaling function fit to all experiments with 1.2< $P_K^{8.89}$ <5.5 GeV/c, including the SciBooNE data, are given in Table IX. The covariance matrix is given in Table X and the correlation matrix is presented in Figure 10.

Table XI lists the differential cross section for the kaon production at the various kaon kinematic points. The uncertainties are obtained as described in Section IV.

Table X gives the covariance matrix for the baseline scaling fit using kaon production data with 1.2< $P_K^{8.89}$ <5.5 GeV/c. The correlation matrix is basically made of two blocks, one associated with the c_1 through c_7 parameters and one associated with the experimental normalization factors. The only coupling of these two sets is through c_1 which has significant correlations with

Scaling Fits	$1.2< P_K^{8.89}(GeV/c) <5.5$		
	Value	Error	
c1	11.29	0.93	
c2	0.87	0.13	
c3	4.75	0.09	
c4	1.51	0.06	
c5	2.21	0.12	
c6	2.17	0.43	
c7	1.51	0.40	Input Error
Aleshin	1.12	0.07	0.10
Allaby	1.07	0.06	0.15
Dekkers	0.87	0.06	0.20
Vorontsov	0.55	0.04	5.00
Abbott	0.79	0.07	0.15
Eichten	1.03	0.06	0.15
χ^2/df (no f)	2.28	$(d.o.f. = 119)$	

TABLE IX. Results for the F-S fits to the K^+ data including a single normalization factor for each experiment and including the two SciBooNE pull term constraints. Error treatment is the same as described in Section III. d.o.f. indicates here degree of freedom and "no f" means no correction factor applied.

the normalization factors. This is expected since the c_1 parameter sets the normalization of the scaling function and should be determined by the data normalizations.

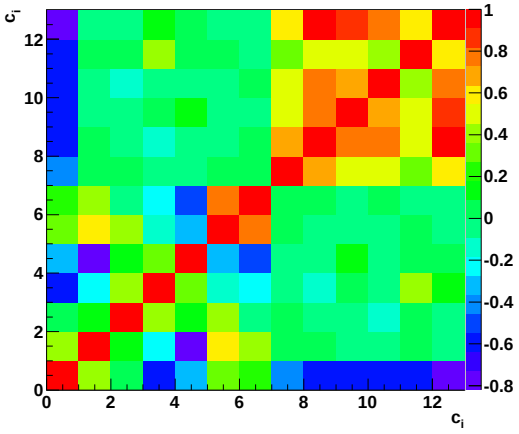

FIG. 10. Correlation for the seven parameters in the F-S fit function and six normalization factor parameters after applying the SciBooNE constraint to the fit due to the K^+ production measurement.

The terms of the covariance matrix from the F-S fit that includes the SciBooNE production measurement include the factor 1.51 for the data set errors rescaling.

The relative uncertainties on the predicted double differential cross section by the F-S fit as function of K^+ angle and momentum decrease including the SciBooNE measurement as shown in Figures 11 and 12.

The SciBooNE measurement confirms the validity of

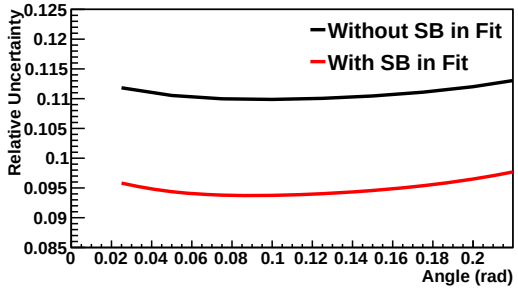

FIG. 11. Relative uncertainty on the double differential cross section as function of K^+ angle ($0.0< \theta_K <0.25$ rad) predicted by the F-S with and without including the SciBooNE production measurement.

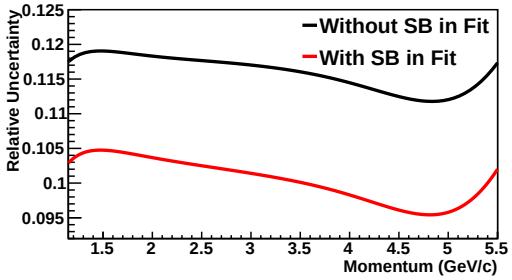

FIG. 12. Relative uncertainty on the double differential cross section as function of K^+ momentum ($1.2< P_K <5.5$ GeV/c) predicted by the F-S with and without including the SciBooNE production measurement.

the F-S parametrization and including the SciBooNE measurement as an additional experimental data to the Feynman Scaling fit contributes in improving both the error uncertainty on the parametrization coefficients and in lowering the total uncertainty in the predicted K^+ production at 8.89 GeV/c proton momentum.

B. SciBooNE K^+ Rate Measurement

In addition to a measurement of K^+ production, the SciBooNE collaboration has also published a measurement of the observed to MC predicted ratio for K^+ produced neutrinos and antineutrinos interacting in the SciBar detector. The results are summarized in Table XII. The SciBooNE rate is the product of the K^+ production and neutrino cross section on carbon as explained in Ref. [22]. Since this result also includes the neutrino interaction cross section, it cannot be directly compared with the other experimental data presented in Table II. This constraint not only covers the neutrino flux from K^+ decay but also constrains the neutrino interaction cross section because the two targets are composed of similar material. The procedure and results for applying the SciBooNE constraint to MiniBooNE is given here since the method is very similar to that used in the K^+

	c1	c2	c3	c4	c5	c6	c7
c1	0.84	0.48E-01	0.39E-02	-0.32E-01	-0.36E-01	0.12	0.69E-01
c2	0.48E-01	0.16E-01	0.14E-02	-0.15E-02	-0.13E-01	0.32E-01	0.22E-01
c3	0.39E-02	0.14E-02	0.73E-02	0.20E-02	0.19E-02	0.14E-01	-0.29E-02
c4	-0.32E-01	-0.15E-02	0.20E-02	0.34E-02	0.20E-02	-0.39E-02	-0.60E-02
c5	-0.36E-01	-0.13E-01	0.19E-02	0.20E-02	0.15E-01	-0.15E-01	-0.24E-01
c6	0.12	0.32E-01	0.14E-01	-0.39E-02	-0.15E-01	0.18	0.12
c7	0.69E-01	0.22E-01	-0.29E-02	-0.60E-02	-0.24E-01	0.12	0.15

TABLE X. Covariance matrix for the seven scaling function fit parameters after applying the SciBooNE production measurements in the F-S fit.

	$P_K^{8.89}$ (GeV/c)	θ_K (rad)	$\sigma_{K\ prod}$ (mb)
$E_\nu = 0.35$ GeV	1.52	0.213	9.05 ± 0.62 (6.9%)
$E_\nu = 0.65$ GeV	2.07	0.127	10.32 ± 0.62 (6.0%)
$E_\nu = 0.90$ GeV	2.45	0.103	9.87 ± 0.58 (5.9%)
Kaon Sweet Spot	2.80	0.106	8.37 ± 0.49 (5.9%)
HE ν_μ Events	4.30	0.055	4.57 ± 0.27 (5.9%)

TABLE XI. Differential cross section values for various kinematic points as in Table V but including in the F-S fit the SciBooNE production measurement for neutrino and antineutrino.

production constraint for the low energy F-S and S-W fits. It should be noted that this analysis is a specific application to MiniBooNE and is not a general result. Nevertheless, the SciBooNE K^+ neutrino rate measurement can be directly applied to MiniBooNE analysis as a constraint on the electron and muon neutrinos from K^+ decay. Electron neutrinos from K^+ decays are one of the important background in the ν_μ to ν_e oscillation search. Understanding this background will result in a reduction of the systematic uncertainty in the MiniBooNE oscillation analysis.

	ν-mode	$\bar{\nu}$-mode	Combined ν+$\bar{\nu}$ mode
K^+ Rate	0.94±0.05±0.11	0.54±0.09±0.30	0.88±0.04±0.10

TABLE XII. K^+ rate measurement results relative to the MC beam prediction for the neutrino, antineutrino, and combined neutrino and anti-neutrino samples. Errors include statistical and systematic errors.

This SciBooNE K^+ rate measurement has been included in a version of the F-S fit and the best fit results for the parameters including the normalization for the data sets is reported in Table XIII. The covariance matrix is reported in Table XIV and correlation matrix is displayed in Figure 13. Table XV lists the differential cross section values for kaon production at several kinematic points.

Scaling Fits	$1.2 < P_K^{8.89}(GeV) < 5.5$ Value	Error	
c1	11.37	0.93	
c2	0.87	0.13	
c3	4.75	0.09	
c4	1.51	0.06	
c5	2.21	0.12	
c6	2.17	0.43	
c7	1.51	0.40	Input Error
Aleshin	1.11	0.07	0.10
Allaby	1.07	0.06	0.15
Dekkers	0.87	0.06	0.20
Vorontsov	0.54	0.04	5.00
Abbott	0.78	0.07	0.15
Eichten	1.03	0.06	0.15
χ^2/d.o.f. (no f)	2.28	(d.o.f. = 119)	

TABLE XIII. Results for the F-S fits as in Figure IX but for the F-S fit results including the SciBooNE rate measurement. d.o.f. indicates here degree of freedom and "no f" means no correction factor applied.

In order to apply the SciBooNE constraint to the MiniBooNE neutrino event prediction, one needs to consider the K^+ kinematic regions that contribute to the two samples.

Figure 9 shows that the kinematic region of K^+ mesons that produce background ν_e events in MiniBooNE and Figure 8 shows the regions that contributes to the SciBooNE rate measurement. While there is a large overlap between the SciBooNE and MiniBooNE regions, the MiniBooNE region extends to somewhat lower K^+ momenta. Using MC studies combined with the covariance matrix associated with F-S fit, we have quantified the increased uncertainty associated with extrapolating the SciBooNE measurement to the lower MiniBooNE region and found that the error on the constrained electron neutrino interaction rate should be increased by a factor of 1.5. This increases the uncertainty for the MiniBooNE electron neutrino event rate prediction from the measured SciBooNE uncertainty of 12% (as reported in Ta-

	c1	c2	c3	c4	c5	c6	c7
c1	0.84	0.47E-01	0.39E-02	-0.31E-01	-0.36E-01	0.12	0.69E-01
c2	0.47E-01	0.16E-01	0.14E-02	-0.14E-02	-0.13E-01	0.32E-01	0.22E-01
c3	0.40E-02	0.14E-02	0.73E-02	0.20E-02	0.19E-02	0.14E-01	-0.33E-02
c4	-0.31E-01	-0.14E-02	0.20E-02	0.34E-02	0.20E-02	-0.38E-02	-0.61E-02
c5	-0.36E-01	-0.13E-01	0.19E-02	0.20E-02	0.15E-01	-0.15E-01	-0.24E-01
c6	0.12	0.32E-01	0.14E-01	-0.38E-02	-0.15E-01	0.18	0.12
c7	0.69E-01	0.22E-01	-0.33E-02	-0.61E-02	-0.24E-01	0.12	0.16

TABLE XIV. Covariance matrix as in Table X but for the F-S fit results including the SciBooNE rate measurement.

	$P_K^{8.89}$ (GeV/c)	θ_K (rad)	$\sigma_{K\ prod}$ (mb)
$E_\nu = 0.35$ GeV	1.52	0.213	9.12 ± 0.62 (6.8%)
$E_\nu = 0.65$ GeV	2.07	0.127	10.39 ± 0.62 (6.0%)
$E_\nu = 0.90$ GeV	2.45	0.103	9.94 ± 0.58 (5.8%)
Kaon Sweet Spot	2.80	0.106	8.43 ± 0.49 (5.8%)
HE ν_μ Events	4.30	0.055	4.60 ± 0.27 (5.8%)

TABLE XV. Differential cross section values as in Table XI but for the F-S fit results including the SciBooNE rate measurement.

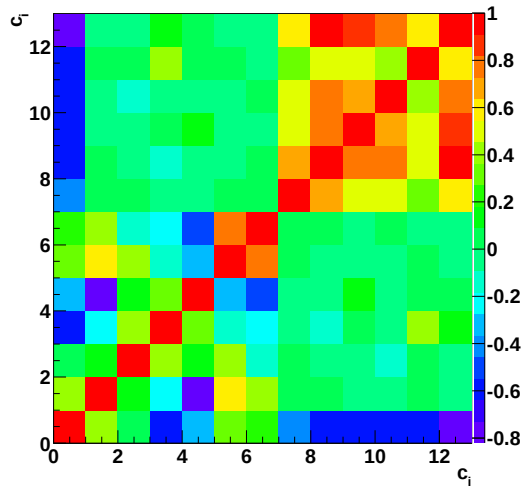

FIG. 13. Correlation between the fit parameters as in Figure 10 but for the F-S fit results including the SciBooNE rate measurement.

ble XII) to a total error of 18%. (The associated covariance matrix given in Table XIV should also have all of the elements multiplied by $(1.5)^2 = 2.25$). After applying the new SciBooNE constraint, the MiniBooNE prediction for electron neutrinos from K^+ decay is reduced by only 3% but the uncertainty is reduced significantly by a factor of three from previous estimates because both the rate and cross section uncertainty is reduced [23].

VII. SUMMARY AND CONCLUSIONS

The F-S parameterization given in Eq. 5 has a theoretically motivated form that takes into account low beam momentum production thresholds from exclusive channels in contrast to many other models. For example, the S-W parameterization does not have the proper scaling properties or expected behavior for the $x_F < 0$ regions. Also, extrapolations using data at much higher beam momentum appear to have difficulty describing lower momentum K^+ production measurements.

The F-S parameterization describes the K^+ production data well for beam momentum in the range of 8.89 to 24 GeV/c. Fits involving different experimental data sets have been performed and show good agreement with the experimental data as shown in Figure 5 where the data have been scaled by the normalization factors given in Table III. The normalization values (except for the Vorontsov data) are in good agreement within the 10% to 20% uncertainties quoted by the experiments.

The F-S fits including the full covariance matrix can be used to predict K^+ production for low beam momentum neutrino experiments such as the BNB at 8.89 GeV/c. The overall uncertainty from the fit is about 7% and is consistent with the combination of the experiments with ∼15% uncertainties. The fits also give the dependence on produced K^+ kinematics in angle and momentum, which is important for accurate neutrino flux predictions using magnetic horn focusing devices.

A cross check of the F-S parameterization using neutrino data from the SciBooNE collaboration measurement reported in Ref. [22] confirms the accuracy of the model at low primary beam momenta and its validity as a better representation of K^+ production with respect to the S-W model. The F-S parameterization derived from the low energy kaon production experiments including this SciBooNE production constraint should therefore be a good representation of K^+ production for low energy neutrino beam simulations. We, therefore, suggest that the parameters shown in Table IX be used along with the covariance given in Table X.

We wish to acknowledge the MiniBooNE and SciBooNE Collaboration for the use of their neutrino simulation programs and the National Science Foundation for the support.

[1] R. P. Feynman, Phys. Rev. Lett. **23**, 1415 (1969).

[2] M. Bonesini, A. Marchionni, F. Pietropaolo, and T. Tabarelli de Fatis, Eur. Phys. J. **C20**, 13 (2001), hep-ph/0101163.

[3] J. W. Norbury, The Astrophysical Journal Supplement Series **182**, 120 (2009), URL `http://stacks.iop.org/0067-0049/182/i=1/a=120`.

[4] J. R. Sanford and C. L. Wang (1967), BNL Internal Report number BNL 11479.

[5] C. L. Wang, Phys. Rev. Lett. **25**, 1068 (1970), URL `http://link.aps.org/doi/10.1103/PhysRevLett.25.1068`.

[6] *SciBooNE experiment*, http://www.sciboone.fnal.gov.

[7] *MiniBooNE experiment*, http://www-boone.fnal.gov.

[8] *MicroBooNE experiment*, http://www.microboone.fnal.gov.

[9] S. E. Kopp, Phys. Rept. **439**, 101 (2007), physics/0609129.

[10] T. Abbott et al. (E-802), Phys. Rev. **D45**, 3906 (1992).

[11] Y. D. Aleshin, I. A. Drabkin, and V. V. Kolesnikov, *Production of $K^{\pm}$ Mesons from Be Targets at 62-Mrad at 9.5-GeV/c Incident Proton Momenta*, ITEP-80-1977.

[12] J. V. Allaby et al., Phys. Lett. **B30**, 549 (1969).

[13] D. Dekkers et al., Phys. Rev. **137**, B962 (1965).

[14] T. Eichten et al., Nucl. Phys. **B44**, 333 (1972).

[15] R. A. Lundy, T. B. Novey, D. D. Yovanovitch, and V. L. Telegdi, Phys. Rev. Lett. **14**, 504 (1965).

[16] G. J. Marmer et al., Phys. Rev. **179**, 1294 (1969).

[17] P. A. Piroué and A. J. S. Smith, Phys. Rev. **148**, 1315 (1966).

[18] I. A. Vorontsov, G. A. Safronov, A. A. Sibirtsev, G. N. Smirnov, and Y. V. Trebukhovsky, *A-Dependence of fragmentation of 9.2-GeV protons on nuclei. (in Russian)*, ITEP-88-011.

[19] F. James and M. Roos, Comput. Phys. Commun. **10**, 343 (1975).

[20] A. A. Aguilar-Arevalo et al. (MiniBooNE), Phys. Rev. **D79**, 072002 (2009), 0806.1449.

[21] F. E. Taylor, D. C. Carey, J. R. Johnson, R. Kammerud, D. J. Ritchie, A. Roberts, J. R. Sauer, R. Shafer, D. Theriot, and J. K. Walker, Phys. Rev. D **14**, 1217 (1976), URL `http://link.aps.org/doi/10.1103/PhysRevD.14.1217`.

[22] G. Cheng et al. (SciBooNE Collaboration), Phys.Rev. **D84**, 012009 (2011), 1105.2871.

[23] E. Zimmerman, in *Proceeding of The 19th Particles and Nuclei International Conference (PANIC11)* (2011).